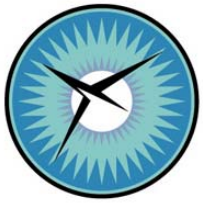

NATIONAL INSTITUTE OF AEROSPACE

Final Report For:
NASA # NNL06AC78T

Task Title:
A Probabilistic Wake Vortex Lateral Transport Model Using Data from SFO and DEN

Prepared by:
George R. Mellman
and
Donald P. Delisi

Task Monitor:
Dr. Fred H. Proctor, NASA Technical Monitor

Reporting Period:
October 2008

NWRA NorthWest Research Associates – www.nwra.com

4118 148th Ave NE, Redmond, WA 98052 Tel: 425.556.9055 Fax: 425.556.9099

NWRA-SEA-08-R365 **3 October 2008**

A Probabilistic Wake Vortex Lateral Transport Model Using Data from SFO and DEN

By

George R. Mellman
and
Donald P. Delisi

Subcontract TO6-6000-NWRA, Subtask 3.1.2

For
NATIONAL INSTITUTE OF AEROSPACE
Dr. David J. Peake, Vice President of Research and Program Development
100 Exploration Way
Hampton, VA 23666-6147

NASA LANGLEY RESEARCH CENTER
Dr. Fred H. Proctor, NASA Technical Monitor
Hampton, VA 23681

Table of Contents

1. Introduction

In a previous report [1], we considered the behavior of the lateral position of vortices as a function of time after vortex formation for Out of Ground Effects (OGE) data for aircraft landing at San Francisco International Airport (SFO). We quantified the spread in lateral position as a function of time and examined how predictable lateral position is under a variety of assumptions. The combination of spread and predictability allowed us to derive probability distribution functions (PDFs) for lateral position given observed crosswind (CW) velocities. In this study, we examine the portability of these PDFs with respect to other landing sites. To this end, we consider OGE data obtained by the Federal Aviation Administration for landings at Denver International Airport (DEN) between 04/05/2006 and 06/03/2006. We consider vortices from both B733 (Boeing 737 models 200-500) and B757 (Boeing 757) aircraft. The data set contains 635 B733 landings and 506 B757 landings. The glide slope altitude for these measurements was 280 m, determined by the average initial vortex observation adjusted for a 3-second delay in the initial observation. The comparable SFO altitude was 158 m.

We note that the principal mechanism for lateral transport in the OGE regime is advection by the ambient wind. This implies that a simple crosswind correction may be effective in explaining much of the variation in the lateral transport data. In this study, we again consider the use of ASOS data and average Lidar crosswind data over the vortex altitude range to predict vortex location as a function of time. These corrections can be truly predictive in that only the wind needs to be measured to predict the vortex evolution. Thus, these corrections could be used operationally to produce probabilities of vortex occurrence as a function of time and measured crosswind velocity. While these constant velocity models provide estimates of residual data scatter, they do not provide information about the source of that scatter. That is, we do not know which part of the data residuals are due to high frequency scatter due to Lidar measurement errors or localized wind variability, which parts are due to the use of inaccurate velocities, which parts are due to non-constant crosswind with altitude, and which parts are due to ground effect. In order to better assess the origins of these effects, we consider an additional model. The linear fit model determines an optimal constant crosswind from the lateral position data for each landing. This model gives the smallest residuals of any constant velocity model, and thus provides a bound on residuals that may be achieved by error-free single velocity estimates. We note that the linear fit model is descriptive, rather than predictive, in that the model uses the lateral position data to derive velocity information.

For each data set and model, we calculate the spread of the residuals of the data minus model estimates. We also compare the difference of the Linear Model crosswinds and the ASOS and Lidar crosswinds as a means of calculating the spread of the data with time. We will then compare the time spread at SFO and DEN as a means of evaluating the portability of the resulting PDFs to other airports.

We note that we have both port and starboard data for many landings. In general, we have more port data than starboard data due to the lidar geometry. Where results are

similar, we present results only for the port data, in the interest of brevity. Unless specifically noted, all plots and results apply to port data.

2. Measurements of Lateral Position

We first consider the B733 data at DEN. The range of the data may be seen in Figure 1. The data clearly shows a linearly increasing spread with time, as may be expected with advection. The data is clearly truncated at about +100 m, which is dictated by the region of interest of the lidar. No truncation is evident for negative lateral positions. We note that this data truncation results in short duration tracks for positive crosswind velocities. This, in turn, results in a spread estimate for the uncorrected position data that is biased low. The uncorrected standard error for the position data is 124m. This value is greater than the 71m measured for the SFO data, reflecting a greater range of average crosswind velocities at DEN. The average Lidar CW velocity range for the SFO data is -8 to 15 kt. The range for DEN is -25 to 15 kt.

A constant velocity crosswind model produces residuals after a correction of the form

$$\delta y(t) = y(t) - v\,t + y(0), \qquad (1)$$

where y is the data as a function of time, v is a measured velocity, determined by ASOS or Lidar or a regression coefficient determined by a linear fit to the lateral position data, and y(0) is the initial vortex position. For this study, y(0) (called y_0 below), which is the lateral position at time t = 0, has been estimated by a regression on the early portion (30 sec) of the lateral position data. We feel that this method is more physically justified than estimating y(0) as a minimum variance solution of ASOS or Lidar corrected residuals, as velocity errors tend to be obscured in the minimum variance case. We do, however, include in selected cases the minimum variance y(0) Lidar model for comparison purposes. We also note that we use a 60 second time window for calculating residuals for our model predictions. This was dictated by the limited time duration of the B733 data and the desire for consistency with the SFO analysis, where ground effects were evident for times greater than 60 seconds.

Figure 2 shows the data residuals after an ASOS crosswind velocity correction has been applied. If the ASOS crosswinds were accurate, the resulting residuals would not increase with time in this figure. Since the residuals do increase with time, it is evident that ASOS velocities do not match the observed lateral position data for a number of landings. Still, the use of ASOS crosswind estimates assuming a fixed y_0 reduces the standard deviation to 62.81 m, a significant reduction. This is, again, greater than the 45.09 m standard error found for the ASOS-corrected data at SFO.

If we consider that ASOS measurements are made at a level 10 m above ground with an instrument located some distance from the observed vortices, it is not surprising that the ASOS estimates do not match the observed position data well. We would anticipate that an average Lidar velocity, which is measured near the location of the

vortices and averaged over the vertical altitudes of the measurements for each landing, would produce better results. This hypothesis, indeed, proves to be the case Using the Lidar line-of-sight velocity averaged over the altitudes where the vortices were measured and using this velocity with a best-fit in eqn. (1) reduces the residual standard deviation to 15.45 m. The Lidar corrections also allow the lateral position at t=0, y_0, to vary in order to minimize variances (called "floating y_0" below). Where velocities do not match the data, this method results in large residuals at the beginning and end of the time series for each landing. These residuals tend to obscure the time dependence of the residual spread. A more appropriate treatment uses the y_0 determined by a linear fit to the early portion (30 sec) of the lateral position data to determine y_0 for each landing. Using y_o determined from a linear fit to the first 30 sec of the lateral position data is called "fixed y_0" below. The residuals are then computed over the entire track using the average Lidar crosswind and the fixed y_0 for each track. The results using these fixed y_0 are shown in Figure 3, and the standard deviation of these residuals is 21.83 m. We note that several landings still stand out very clearly in this figure as having substantially incorrect velocities. We also note that the results for in Figure 3 show a clear increase in variance with time. Once again, these residual standard errors are greater than those that were determined for SFO of 10.59 m and 14.81 m, for floating and fixed y_0, respectively.

Instead of using the average Lidar crosswind, we can determine an optimal constant crosswind by performing a linear regression on the first 60 seconds of lateral position data for each landing. This method is called the Linear Model. For fixed y_o, we still use the first 30 seconds of data to determine y_o for each track. Now, however, the optimal constant crosswind is found by a linear regression on the first 60 seconds of lateral position data. The residuals are then computed using y_o and this optimal constant crosswind The residuals for this model are shown in Figure 4. The standard deviation for the data in Figure 4, using the Linear Model, is 8.32 m. This value is significantly smaller than the Lidar residual of 21.83 m, but, once again, larger than the comparable Linear Model residual standard error of 7.13 m found for SFO. The small residuals using the Linear Model suggest that the effects of vertical inhomogeneity in the crosswinds are rather small for the B733 lateral transport dataset at both SFO and DEN. The relative sizes of the residuals for the Lidar and Linear Model corrections suggest that about half of the Lidar residuals are attributable to velocity errors, with the other half attributable to the presence of high frequency noise and deviations from a constant crosswind velocity. We note that the residuals for the Linear Model do not show an obvious increase with time, implying that the Linear Model is a good representation of the data behavior over the analysis window. The Linear Model is not, however, predictive in that it requires lateral position measurements to predict the lateral transport.

In order to explore the systematic discrepancy between SFO and DEN residuals, we examine the lidar residuals vs time as a function of the average lidar velocity for DEN, as shown in Figure 5. We note that, except for the few tracks at the highest negative CW velocities, there does not appear to be a strong trend of residual amplitude with CW velocity. This suggests that the larger residuals at DEN are not related to the greater CW velocity spread. A comparison of the Linear Model residuals as a function of time at DEN and SFO suggests that the Linear Model residuals are larger at DEN due to

greater high frequency scatter. The difference in Linear Model residuals is too small, however, to explain the changes in the ASOS and Lidar residuals. Similarly, limiting the time duration of the data appears to have little effect on the residuals. The absence of sufficiently large pointwise residuals and the relative insensitivity to time duration suggests that DEN has somewhat greater errors in the ASOS and Lidar CW velocities relative to the optimal constant CW velocities. We suspect that these larger errors are due to the greater range in crosswind velocities at DEN and the lower Lidar signal-to-noise ratios at DEN.

An examination of the confidence limits on the Linear Model regression coefficients for the DEN data set show that the resulting uncertainty in CW velocity estimates has a strong dependence on the number of points (or, alternatively, the track duration). The median standard error, as a function of the number of points present, is shown in Table 1.

Table 1. Regression Error in CW Estimates as a Function of the Number of Data Points in the Port Vortex Track

Number of Data Points	Regression (kt)
3	2.50
4	1.54
5	1.00
6	.74
7	.58
8	.46
9	.36
10	.30
11	.26
12	.22

If we wish to have a meaningful comparison of Lidar and Linear Model CW velocities, we must restrict the data such that the uncertainty in the Linear Model estimates is less than the difference between the Linear Model and Lidar estimates. The data shows that the number of data points has little effect on the point-wise residual errors of the Linear Model and Lidar corrected residuals. However, it has a significant effect on our ASOS residuals and on the final PDFs. The effect on residuals is shown in Table 2.

Table 2. Effect of Data Restrictions on Standard Errors

Residual		Standard Error(m)
Linear Model Residuals	- NP>2	9.12
	- NP>6	8.79
	- NP>8	8.80

Lidar Residual Float Y_0	- NP>2	15.44
	- NP>6	14.51
	- NP>8	14.32
Lidar Residual Fixed Y_0	- NP>2	21.83
	- NP>6	21.83
	- NP>8	21.89
ASOS Residual Fixed Y_0	- NP>2	62.81
	- NP>6	76.94
	- NP>8	82.73

where NP is the number of data points required in each track.

We note that the elimination of short tracks results in an attendant decrease in the number of landings available, as shown in Table 3.

Table 3. Effect of Data Restrictions on the Number of Landings

DEN		NP>1	NP>3	NP>6
	B733	629	467	172
	B757	465	465	261
SFO		NP>1	NP>3	NP>6
	B733	459	455	379
	B757	480	480	454

From Table 1, we note that the regression error drops below the estimated standard deviation of the Linear minus Lidar CW velocities found in [1] for SFO (.90 kt) for NP>6. We feel that NP>6 represents a good tradeoff between the number of tracks available (reduced from 629 to 172 for the B733 at DEN) and the standard error of the regression coefficients, and we have used NP>6 for all DEN comparisons. Operationally, the reduction of runs for NP>6 should not be important, since just weaker and/or rapidly decaying wakes have been eliminated. We note, however, that only longer lasting vortices have been retained. Hence, wake lifetimes are biased in these results. For NP>6, the Linear Model crosswind estimates agree well with the average Lidar estimates, as shown in Figure 6 . The comparison of the Linear Model and ASOS crosswind estimates, shown in Figure 7, shows considerably more scatter. The Lidar and ASOS comparison, shown in Figure 8, shows scatter comparable to the Linear Model vs ASOS plot (Figure 7).

As we did in [1], we can model the time dependent distribution of Lidar and ASOS residuals in terms of a constant distribution of the Linear Model residuals, an explicit time term, and the distribution of Linear Model CW velocity estimates minus Lidar or ASOS CW velocity estimates. The Lidar residuals, for instance, are given by

$$\delta y_{Lidar} = y - v_{Lidar} t \,. \qquad (2)$$

We can rewrite this as

$$\delta y_{Lidar} = y - \left(v_{Lidar} - v_{LM}\right) t - v_{LM}\, t \tag{3}$$

or

$$\delta y_{Lidar} = \delta y_{LM} - \left(v_{Lidar} - v_{LM}\right) t \tag{4}$$

We thus express the distribution of the Lidar residuals in terms of the Linear Model residual distribution, which we recall is independent of time, and the velocity difference distribution. If we assume Gaussian distributions, we find the covariance of the Lidar residuals is given by

$$C\left(\delta y_{Lidar}, \delta y_{Lidar}\right) = C\left(\delta y_{LM}, \delta y_{LM}\right) + C\left(\delta v, \delta v\right) t^2 - 2C(\delta y_{LM}, \delta v)\, t \tag{5}$$

The correlation coefficient of the velocity difference and the Linear Model residual is 0.01, effectively eliminating the cross-correlation term. The time variation of the standard deviation of the Lidar residual is thus given by the t^2 term. A similar treatment applies for the ASOS residuals.

Figure 9 shows the distribution of Linear Model CW velocity estimates minus average Lidar CW velocity estimates. The standard deviation of 1.15 kt for the DEN B733 data with NP>6 is greater than the estimate of 0.90 kt for comparable SFO data, but is still quite small. Figure 9 may be compared to a similar plot for SFO data shown in Figure 10. Figure 11 shows the distribution of Linear Model CW velocity estimates minus average ASOS CW velocity estimates for the B733 OGE measurements at DEN with NP>6. The standard deviation of 3.87 kt. for the DEN B733 data with NP>6 is significantly greater than the estimate of 2.66 kt for comparable SFO data and is sufficiently large to make the ASOS measurements of limited utility as a surrogate for crosswind at altitude and as a predictor of lateral position. The similar plot for SFO data is shown in Figure 12.

We have performed a similar analysis for Boeing 757 landings at DEN to test whether lateral transport models are consistent between aircraft. We have again chosen to limit our data set to times less than 60 seconds and landings with more than 6 points to insure compatibility between the B733 and B757 data sets at both DEN and SFO, due to the limited duration of the B733 data and the onset of ground effects at SFO. We find that the B757 results and the B733 results show good agreement for lateral position prediction. Figure 13 shows the raw lateral transport data for the port vortex. We note that the data is similar to the B733 data except for the greater duration of the B757 vortices, which is a result of the stronger vortices from the B757. As in Figure 1, we again note the same ROI limitations at 100 m as noted in the B733 data. The standard

deviation of the raw B757 data for t<60 s is 111.3 m, compared to 124 m, for the B733 DEN data. The ASOS corrected B757 data, shown in Figure 14, has a standard error of 64.79 m, compared to 62.81 m, for the DEN B733 data. The Lidar corrected residuals with y_0 constrained, shown in Figure 15 for the DEN B757 data, has a standard error of 23.27 m, compared with 21.83 m, for the B733 data at DEN. The standard error of the Linear Model residuals for the DEN B757 data, shown in Figure 16 is 7.83 m, compared to 8.32 m, for DEN B733 data. The Linear Model residuals are again largely independent of time over the analysis window, as opposed to the obvious time spread of the ASOS and Lidar corrected residuals.

The distributions of Linear Model CW minus average Lidar or ASOS CW estimates are also consistent between the B757 and B733 data for DEN. For Linear Model minus average Lidar, the standard deviation is 1.20 kt for the B757 data versus 1.15 kt for the B733 data at DEN. For the Linear Model CW minus ASOS CW, we find a standard deviation of 3.67 kt for the B757 versus 3.87 kt for the B733.

3. Comparison of SFO and DEN Model Results

We have attempted to be consistent in our choice of time windows and models to best compare both aircraft and landing sites. To this end, we have used a time window of 60 seconds beyond the first vortex observation for each track. This is dictated by the duration of the B733 data and the onset of near ground effects at SFO for the B744 and B757 data. We have also restricted all data to only those tracks containing at least 7 points. Lidar and ASOS corrections were performed using a fixed y_0. However, in order to enhance precision, residuals for the Linear Model, use a floating y_0. The original SFO models used y_0 determined from an inversion procedure. This gives systematically slightly different residuals than a y_0 determined from a short duration linear fit to the data. The difference is only about 1 m, but this is large enough to blur differences between the sites. In order to consistently compare SFO and DEN results, we therefore use the floating y_0 determined by regression for each track in this section.

The standard errors for all lateral position models, using a fixed y_0 except for the Linear Model results, are shown in Table 4.

Table 4. Standard Errors for Lateral Position Models

	SFO B733	SFO B757	SFO B744	DEN B733	DEN B757
RESIDUALS (RMS)					
Raw Data (60 s)	71.2 m	56.5 m	66.5 m	124.0 m	111.3 m
ASOS Corrected	45.1 m	38.4 m	42.5 m	62.8 m	64.8 m
Lidar Corrected	14.8 m	14.1 m	15.5 m	21.8 m	23.3 m
Linear Model (float)	5.2 m	5.5 m	5.3 m	8.3 m	7.8 m

CW VELOCITY RESIDUALS					
Linear Model- Lidar	0 .91 kt	0.83 kt	0.89 kt	1.14 kt	1.20 kt
Linear Model-ASOS	2.70 kt	2.40 kt	2.70 kt	3.90 kt	3.70 kt

Table 4 illustrates that all residuals considered show much greater variation between landing sites than they show between aircraft types. For the raw lateral position spread, this is easily explained by the greater range in crosswind velocities at DEN compared to SFO. Other residuals, however, do not show strong correlation with crosswind. Table 5, for example, shows the residuals of Linear Model CW velocities minus average Lidar CW velocities for 5 kt Lidar CW bins for B757 landings at DEN. Variations in standard deviation are not statistically significant for crosswind speeds less than 15 kt. Differences for crosswind speeds greater than 15 kt are statistically significant, despite having a smaller number of tracks. This result is typical of other residual measures where sufficient data is available to perform this analysis. A similar result is found for B733 aircraft at DEN. While SFO does not show sufficient CW velocity range to allow this same analysis, a comparison of residuals from positive and negative Lidar CW velocities, corresponding to winds off land and off the Bay, shows virtually no difference in Linear Model minus Lidar CW velocity residuals.

Table 5. Linear Model Cw Velocity Minus Lidar Cw Velocity by 5kt Cw Bins for Den B757

AVERAGE LIDAR CW BIN	STANDARD DEVIATION LINEAR MODEL-LIDAR CW	# TRACKS
CW> 5 kt	1.12 kt	15
0< CW< 5 kt	1.20 kt	59
-5< CW< 0 kt	1.19 kt	80
-10<CW< -5 kt	1.14 kt	51
-15<CW<-10 kt	1.10 kt	21
-20<CW<-15 kt	2.05 kt	11
CW<-20 kt	2.43 kt	4

We note that variation of residuals for different aircraft at the same site are typically about 10% while variations for common aircraft types at different sites are 30% to 50%. Residuals at DEN are consistently larger than those at SFO. Analysis of Variance shows that the differences between sites are statistically significant at greater than a 95% confidence level. The causes of the site differences are not clear at this time. Candidates for the site differences include differences in initial vortex altitude at the two sites (274 m, at DEN vs 156 m, at SFO), deviations from a constant CW velocity, and atmospheric differences.

We can explore the effects of altitude variation in the crosswinds by examining the standard error of the residuals for the Linear Model. This error is approximately 5.3

m for SFO and 8 m for DEN. In neither case do we see appreciable spreading of the residuals with time. We would like to know whether the residuals are dominated by the assumption of constant CW velocity with altitude or whether they represent high frequency errors in either vortex position or localized variability in CW velocity. To explore this issue, we compare residuals from linear, quadratic, and cubic fits for Linear Mixed Effects models for lateral position as a function of time. The results are given in Table 6.

Table 6. Lateral Position Residuals for Polynomial Fits

	LINEAR	QUADRATIC	CUBIC
SFO B733	5,18 m	4.57 m	4.41 m
SFO B744	5.27 m	4.66 m	4.49 m
SFO B757	5.48 m	4.33 m	4.10 m
DEN B733	8.32 m	7.69 m	7.68 m
DEN B757	7.83 m	7.00 m	6.91 m

Table 6 shows that, for a given aircraft at either SFO or DEN, the residuals decrease as the order of the fit increases from linear to cubic. However, the reduction from the linear to the quadratic fit is small, and the reduction from the quadratic to the cubic fit is very small. These results suggest that relatively little of the residual results from large CW velocity gradients, but, rather, from either high frequency variability in the crosswinds or random location errors in the lateral position measurements. The results are remarkably consistent over aircraft types and show a definite difference between SFO and DEN landing sites. In future work, we will explore the effects of Lidar signal to noise ratio and Lidar CW velocity variability as a function of time and altitude as a means of explaining landing site variability.

Despite systematic differences between landing sites, the results obtained in [1] still apply qualitatively to DEN. Residuals for the Linear Model are small and time independent. The Lidar residuals are larger than the Linear Model residuals and show an increased spread with time, but are still small enough to have predictive utility. The ASOS residuals are large, show a clear linear spread increase with time, and are too large to have much predictive utility. In the next section, we compare the effects of site differences on the cumulative probability distributions for lateral position.

4. Probability Distributions of Lateral Position

In this section we construct probability density functions (PDFs) for lateral position as a function of time for each landing site and each aircraft type. As in our earlier report [1], we make use of equation (5) to construct the PDFs from the time independent Linear Model residuals and the distribution of CW velocity differences between the Linear Model and the measured ASOS or Lidar data. This method of estimating PDFs avoids possible bias due to the correlation of track duration with

crosswind velocity. Figure 17 shows the distributions of the differences between Linear Model CW velocity and average Lidar CW velocity for B733 and B757 aircraft at DEN and SFO averaged over all Lidar CW velocities. Figure 18 shows the resulting cumulative PDFs as probability contours for a zero knot CW velocity. Figure 18a shows the PDFs for B733 OGE aircraft, and Figure 18b shows the PDFs for B757 aircraft. The broader velocity distributions at DEN clearly result in somewhat broader PDFs. Figures 19 and 20 show the velocity error distributions and PDFs for ASOS crosswinds. The PDFs for ASOS corrected lateral positions are clearly broader than those for Lidar corrected lateral positions. Table 7 shows the 95% confidence limits for Lidar and ASOS PDFs.

Table 7. 95% Confidence Limits at 60 Seconds

	LOWER LIMIT	UPPER LIMIT
DEN B733 LIDAR	-69 m	69 m
DEN B757 LIDAR	-73 m	73 m
SFO B733 LIDAR	-54 m	54 m
SFO B757 LIDAR	-50 m	50 m
DEN B733 ASOS	-206 m	206 m
DEN B757 ASOS	-234 m	234 m
SFO B733 ASOS	-162 m	162 m
SFO B757 ASOS	-144 m	144 m

This table clearly shows the utility of lidar measurements as a predictor for lateral position. Equally clear is the lack of predictive utility for the ASOS measurements.

We may also construct PDFs for other crosswind velocities. Figure 21 shows the PDFs for a range of crosswind velocities for DEN B757 data. In these plots, we have used the correct estimated standard errors for a 5 kt bin surrounding the assumed crosswind velocity. The PDFs clearly show the advection effects superimposed on the velocity uncertainty effects.

5. Summary

In this study, we have attempted to quantify the intrinsic error in lateral position data for DEN OGE data, as well as examining the utility of ASOS and Lidar crosswind estimates for predicting lateral vortex position as a function of time. We found that the intrinsic variability of lateral position OGE data, estimated using regression models, is small, on the order of 7 to 8 m. The use of Lidar CW estimates to predict vortex lateral position shows both random and time varying errors. The time varying errors may be interpreted as CW velocity errors with a standard error of about 1.2 kt. This error is small enough to allow, we believe, operational use of Lidar CW as a predictor of lateral position. The use of ASOS CW as a predictor shows both random and time dependent errors. Using ASOS CW, the velocity error is about 3.8 kt, which is large. This large

error may not allow operational use of ASOS as a predictor of crosswind. The results are quite similar for B733 and B757 aircraft types.

The DEN results are qualitatively similar to results previously obtained for SFO. The SFO results show consistently less random and velocity scatter. These differences are statistically significant but are not large enough to change the operational utility of the methods.

References

[1] Mellman, G.R. and D.P. Delisi,. Status Report on a Probabilistic Wake Vortex Lateral Transport Model, NWRA Report NWRA-BELL-05-R355, Bellevue, WA, 2007.

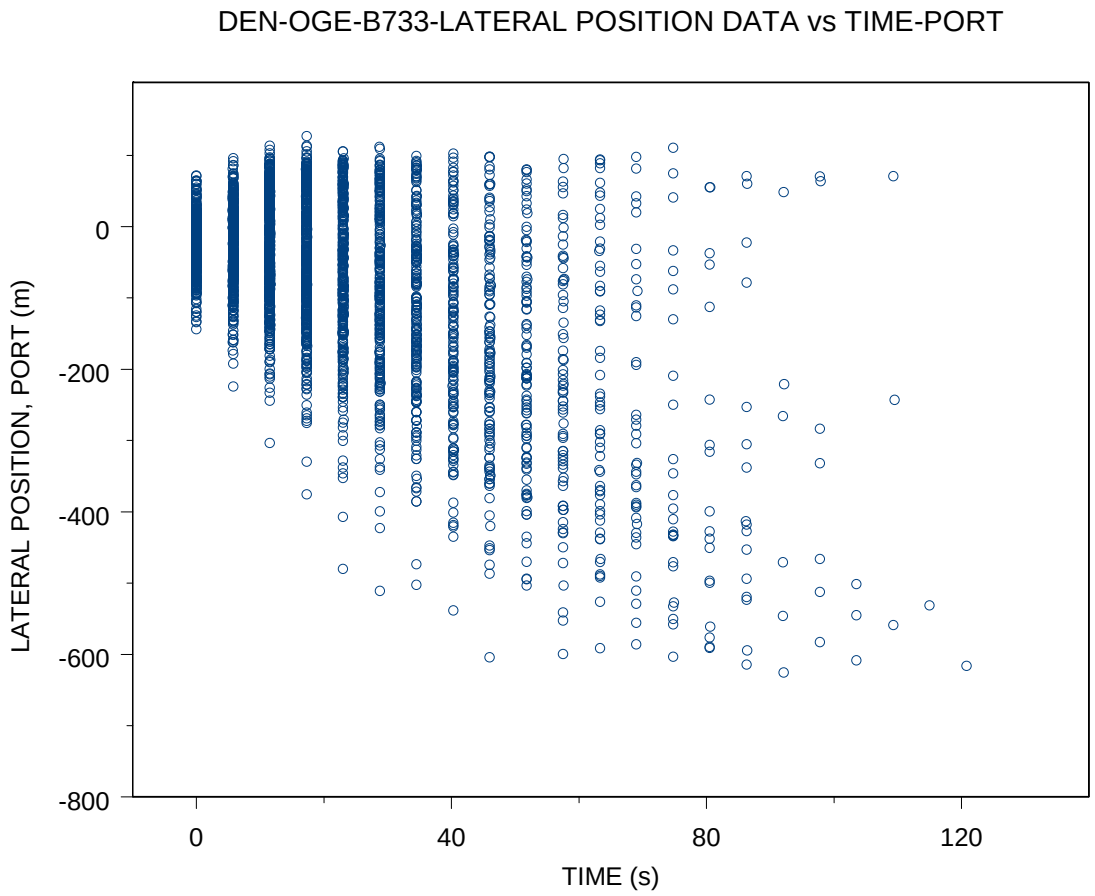

Figure 1. Lateral position data for DEN as a function of time for all B733 OGE landings at DEN. The standard error is 124 m.

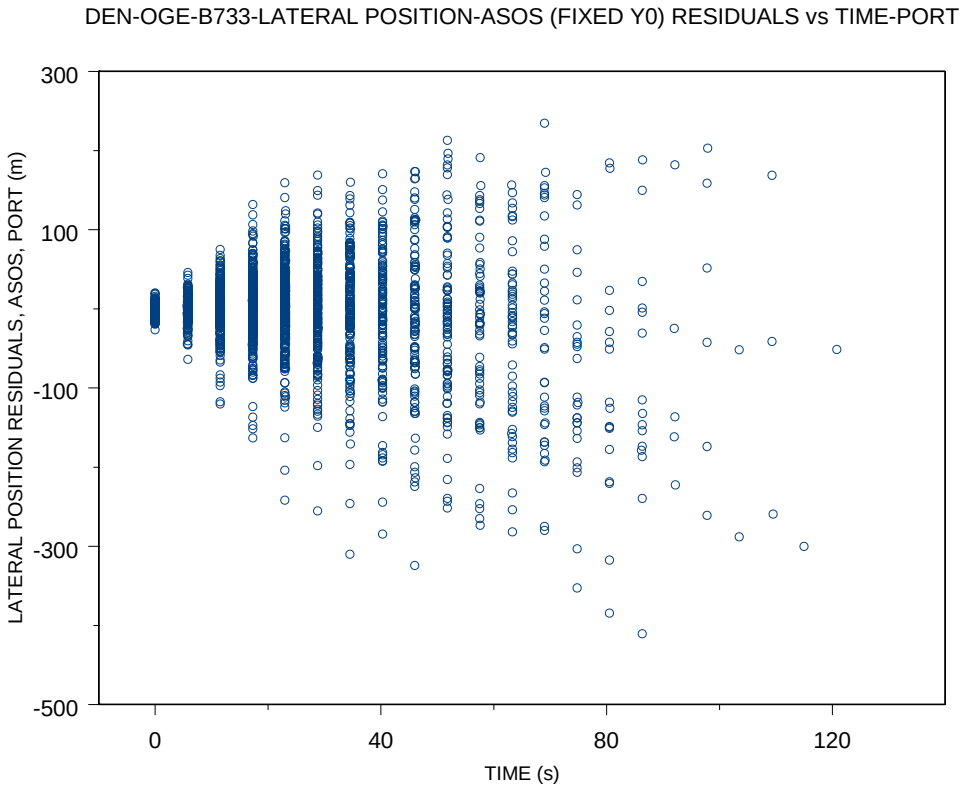

Figure 2. Lateral position residuals using ASOS crosswind, for all B733 OGE landings at DEN with more than 7 points in the port track. For each landing, y_0 was fixed using a 30 s linear estimate. The standard error is 62.8 m.

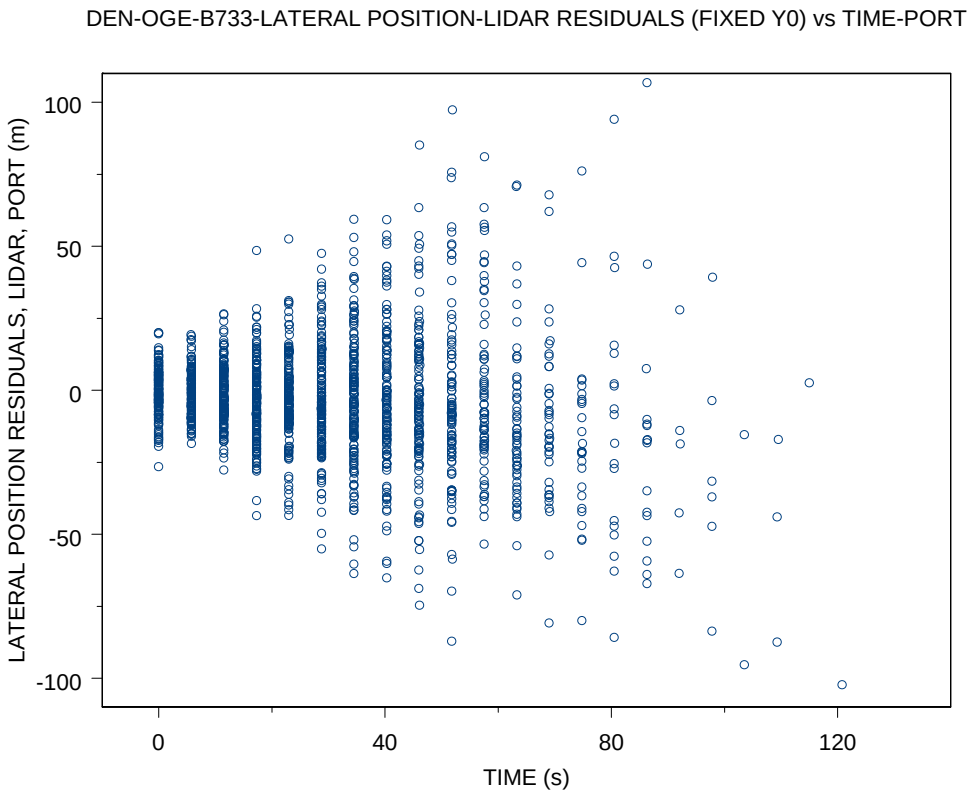

Figure 3. Lateral position residuals using average Lidar crosswind, for all B733 OGE landings at DEN with more than 7 points in the port track. For each landing, y_0 was fixed using a 30 s linear estimate using lateral position data.. The standard error is 21.8 m.

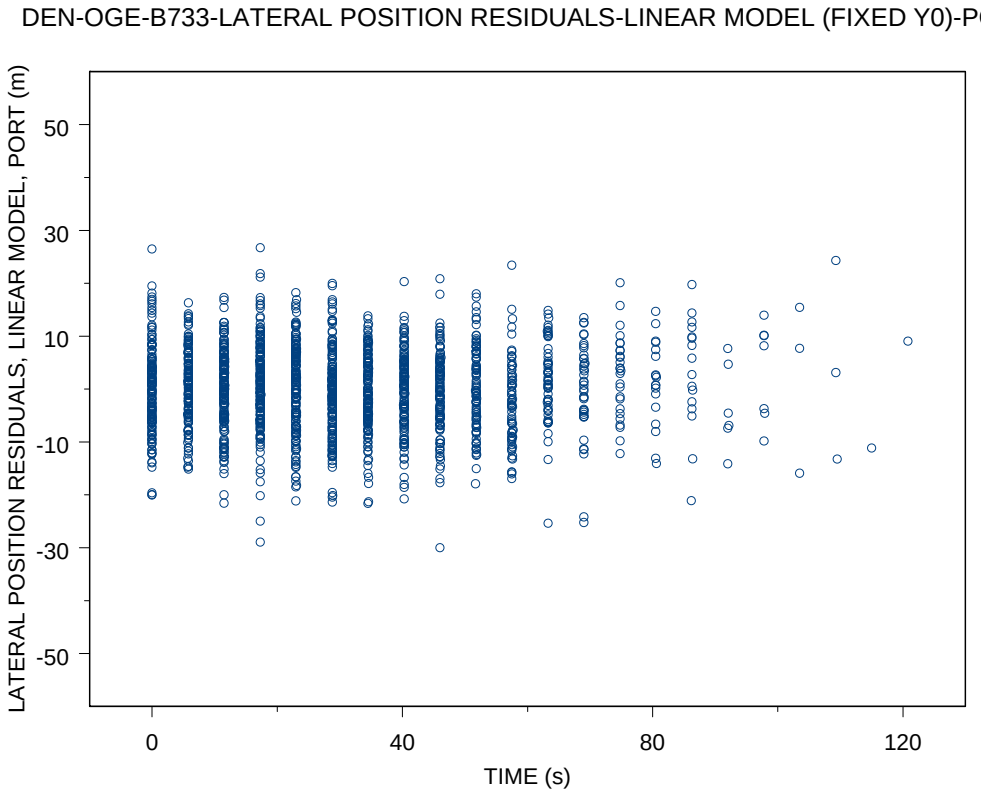

Figure 4. Lateral position residuals using the optimal constant crosswind (the Linear Model) and fixing y_0 for each landing using a 30 s linear fit to lateral transport data for B733 OGE landings at DEN with at least 7 data points in the port track. Note the time independence of the residual spread. The standard error is 8.3 m.

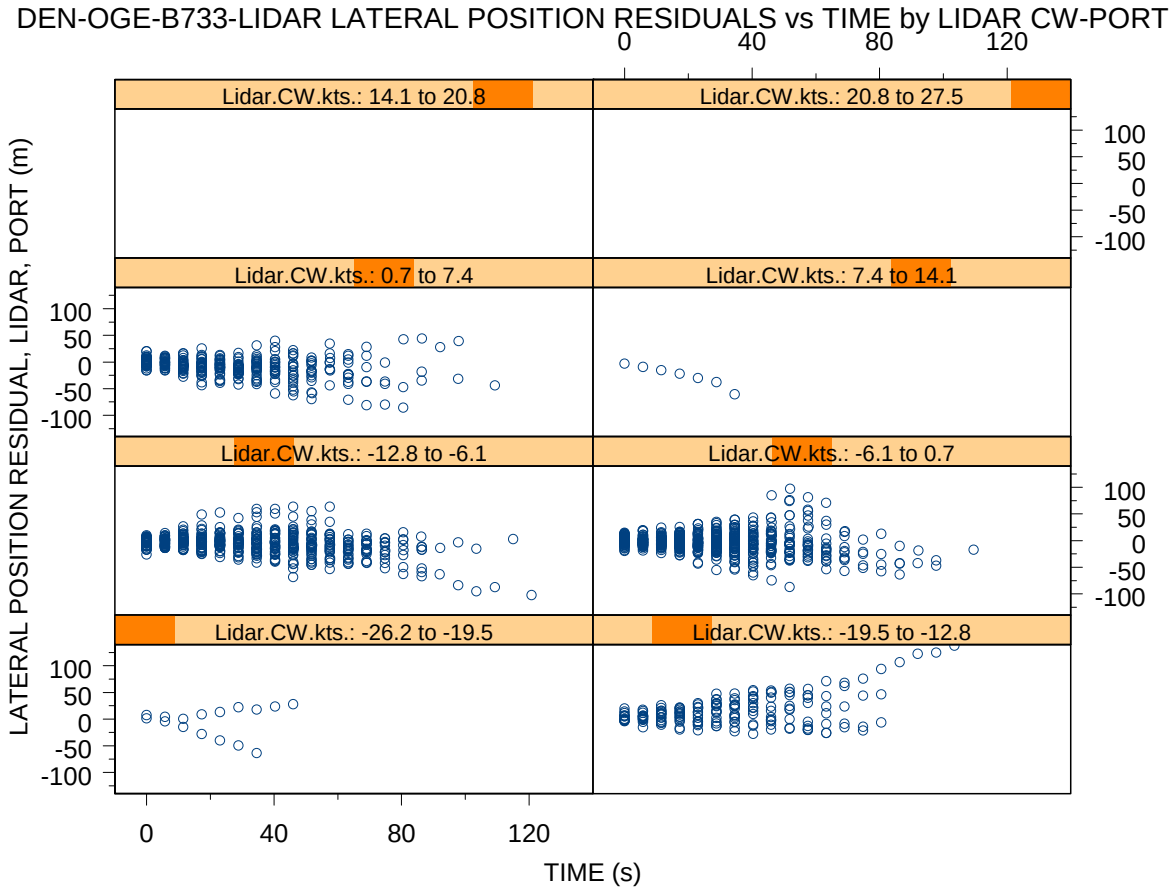

Figure 5. Lateral position residuals using the average Lidar crosswind correction grouped by average Lidar crosswind velocity for all B733 OGE landings at DEN with at least 7 data points in the port track. Note that the spread appears independent of crosswind velocity.

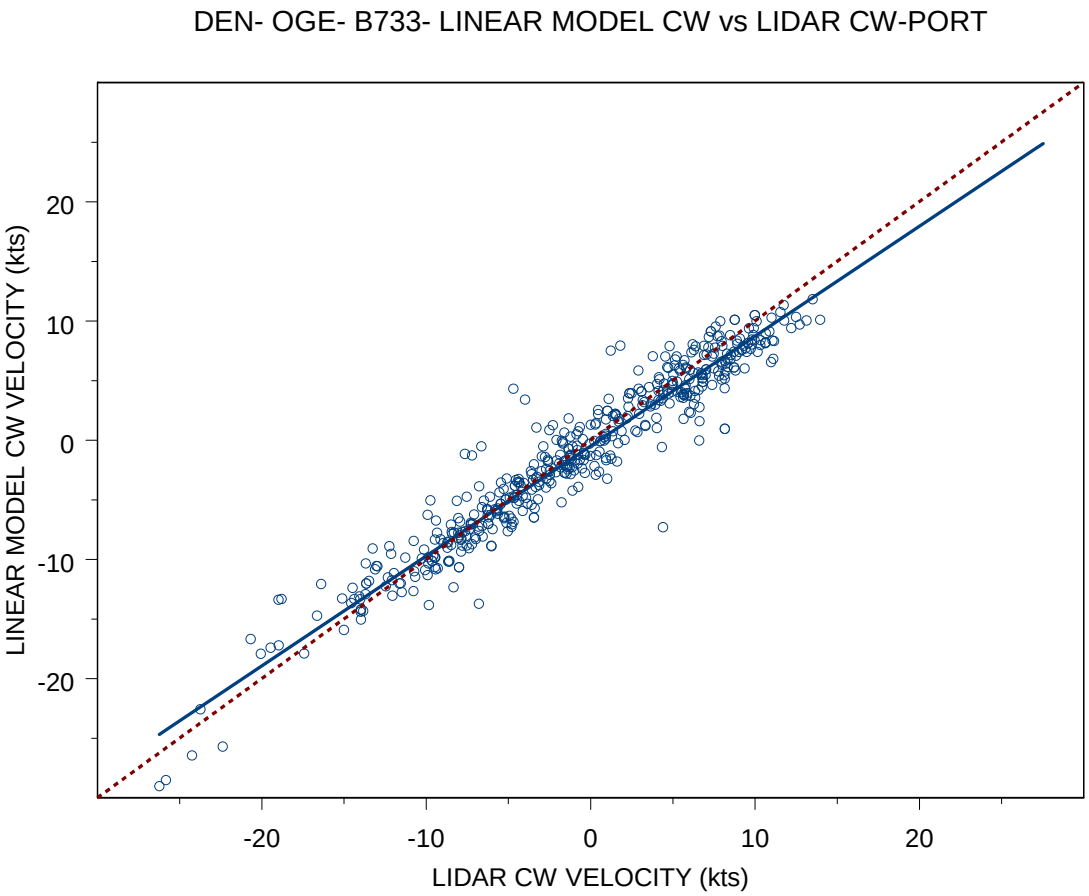

Figure 6. Comparison of the Linear Model crosswind with the average Lidar crosswind for all B733 OGE landings at DEN with at least 7 data points in the port track.. The solid line is the least squares fit to the data while the dashed line is a reference line with unit slope.

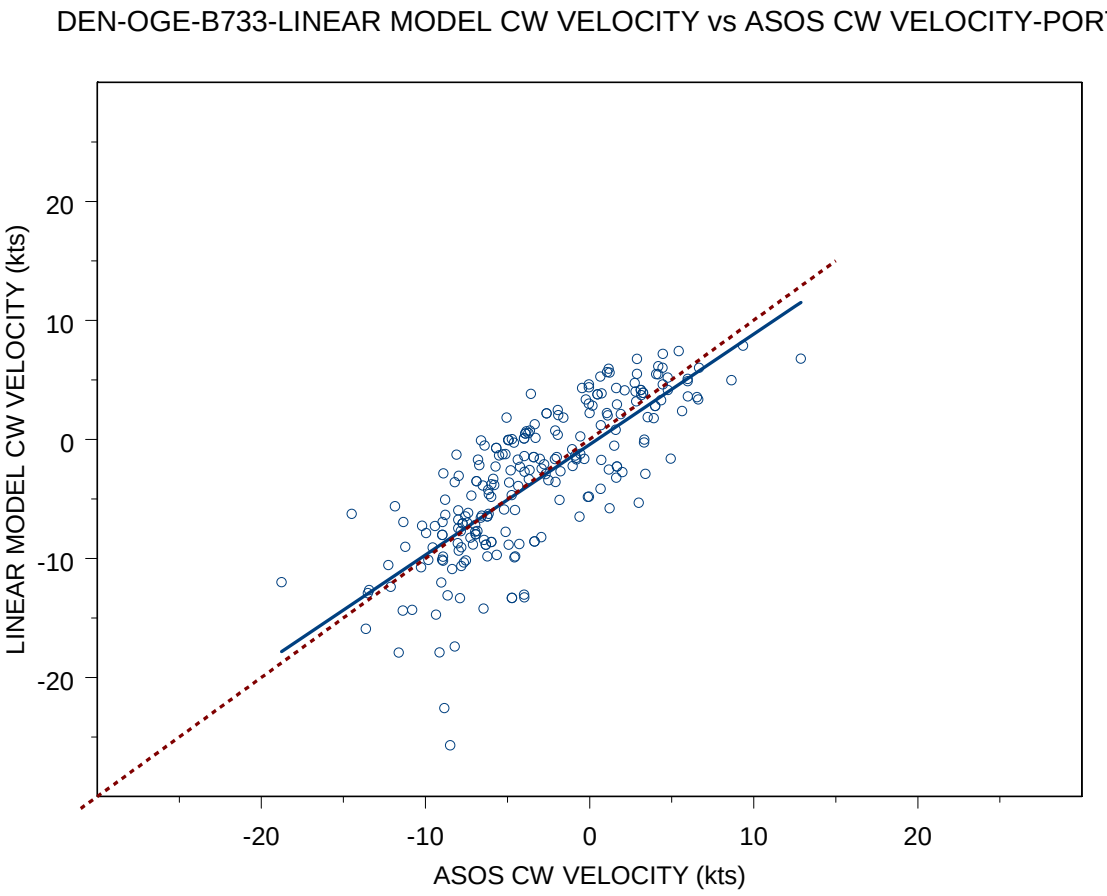

Figure 7. Comparison of Linear Model crosswind with ASOS crosswind for all B733 OGE landings at DEN with at least 7 data points in the port track. The solid line is the least squares fit to the data, while the dashed line is a reference line with unit slope.

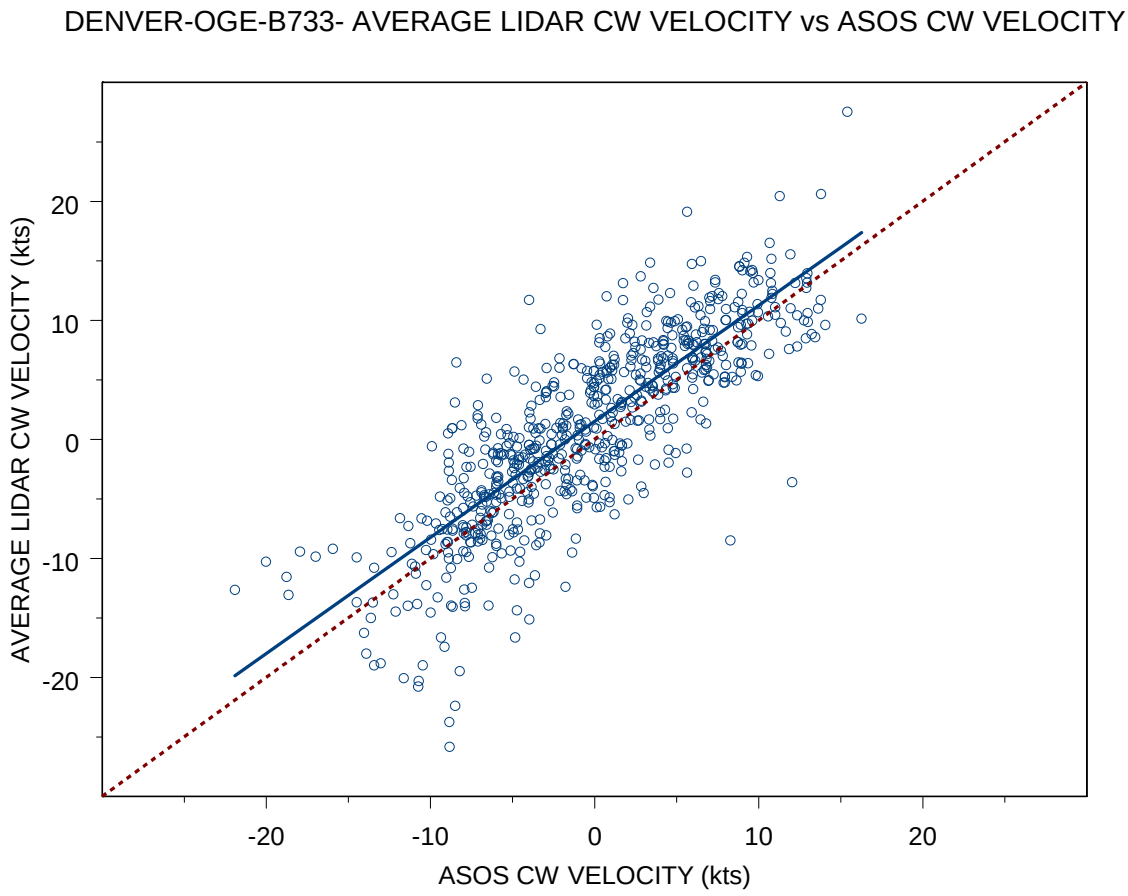

Figure 8. Comparison of ASOS crosswind with average Lidar crosswind for all B733 OGE landings at DEN. The solid line is the least squares fit to the data, while the dashed line is a reference line with unit slope.

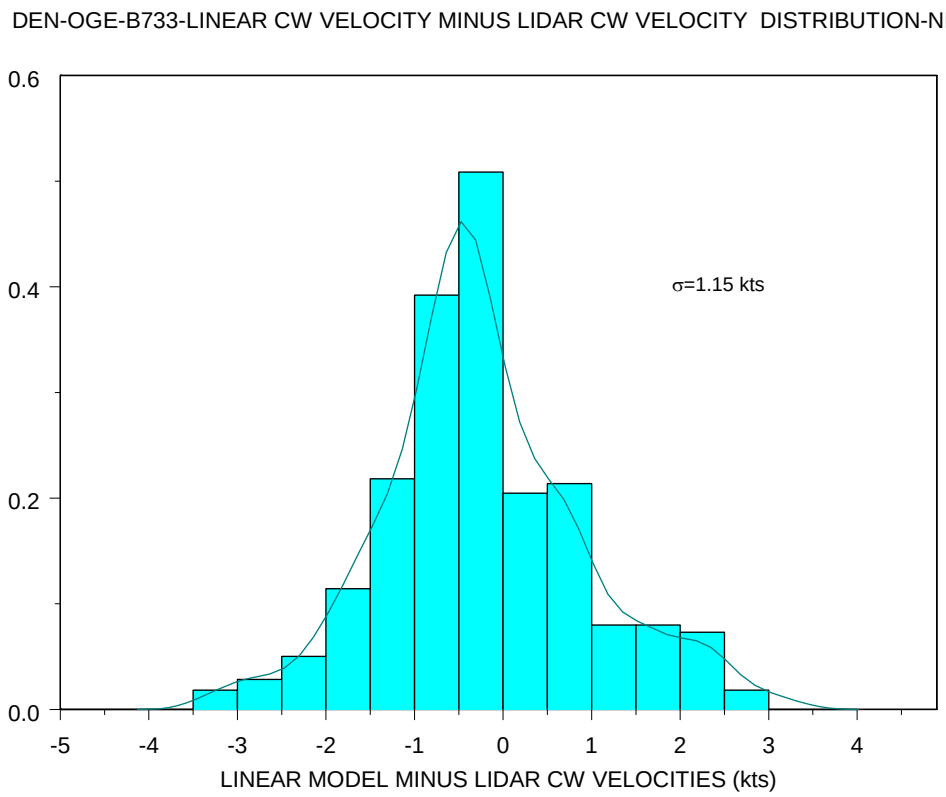

Figure 9. Probability distribution of the difference between the crosswind from the Linear Model and the average Lidar crosswind for all B733 OGE landings at DEN with at least 7 data points in the port track. 172 landings were used in this plot. The standard deviation of the distribution is 1.15 kt.

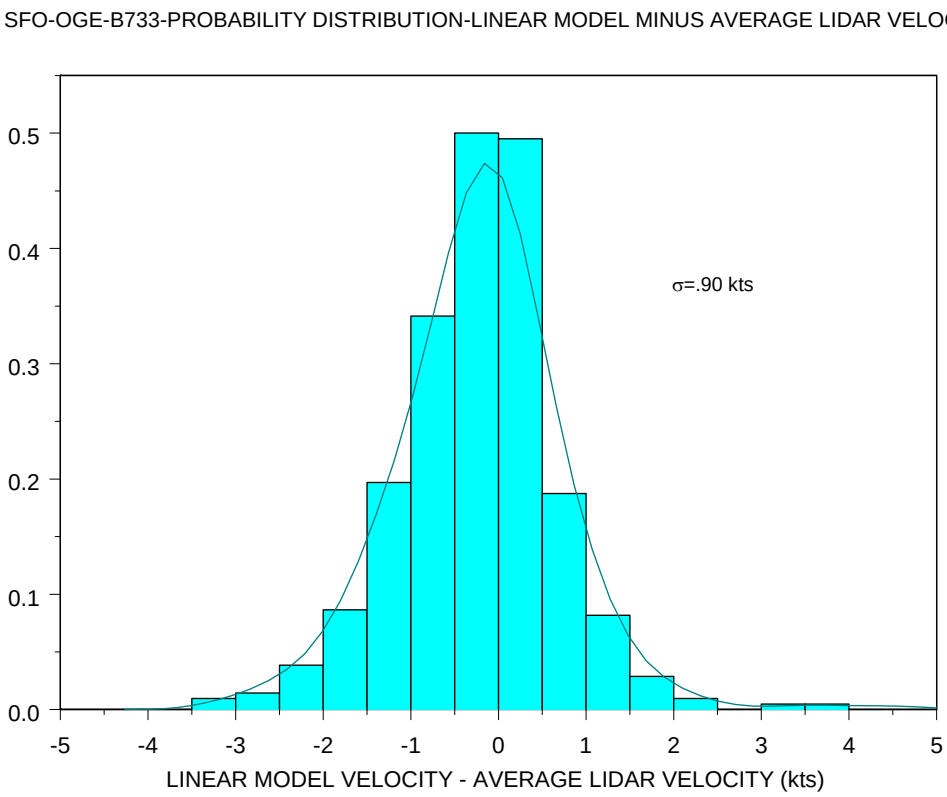

Figure 10. Same as Figure 9, but for SFO. 379 landings were used in this plot. The standard deviation of this distribution is 0.90 kt.

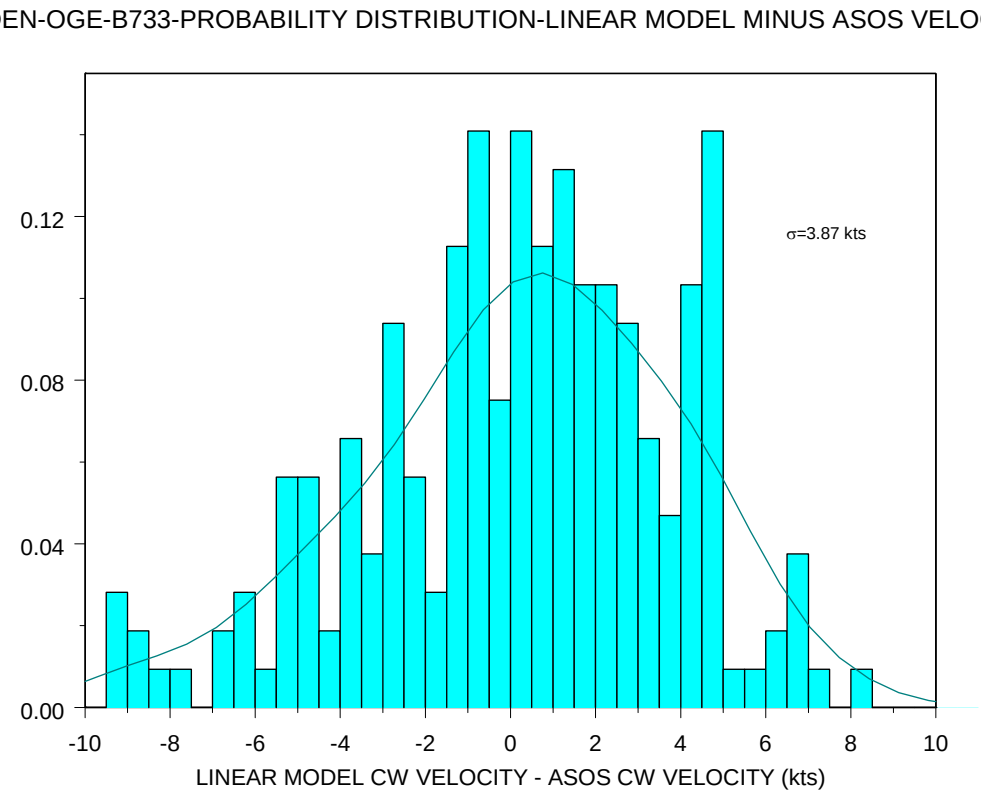

Figure 11. Probability distribution of the difference between the crosswind from the Linear Model and the ASOS crosswind for all B733 OGE landings at DEN with at least 7 data points in the port track. The standard deviation for this distribution is 3.87 kt, which is substantially larger than the 1.15 kt in Figure 9.

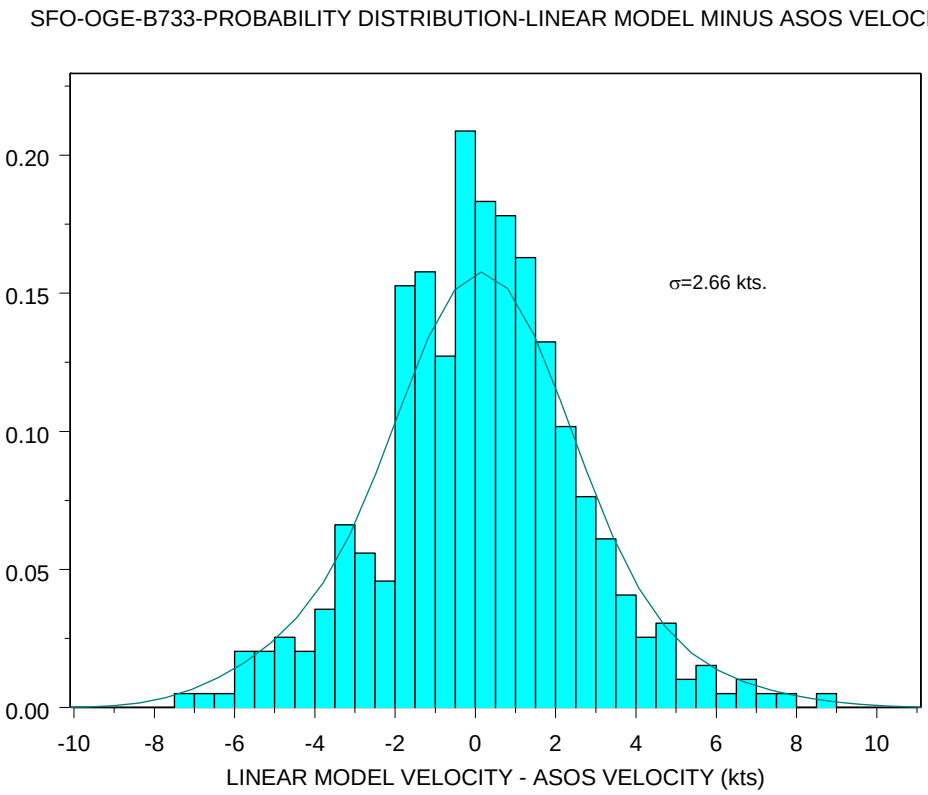

Figure 12. Same as Figure 11 but for SFO.

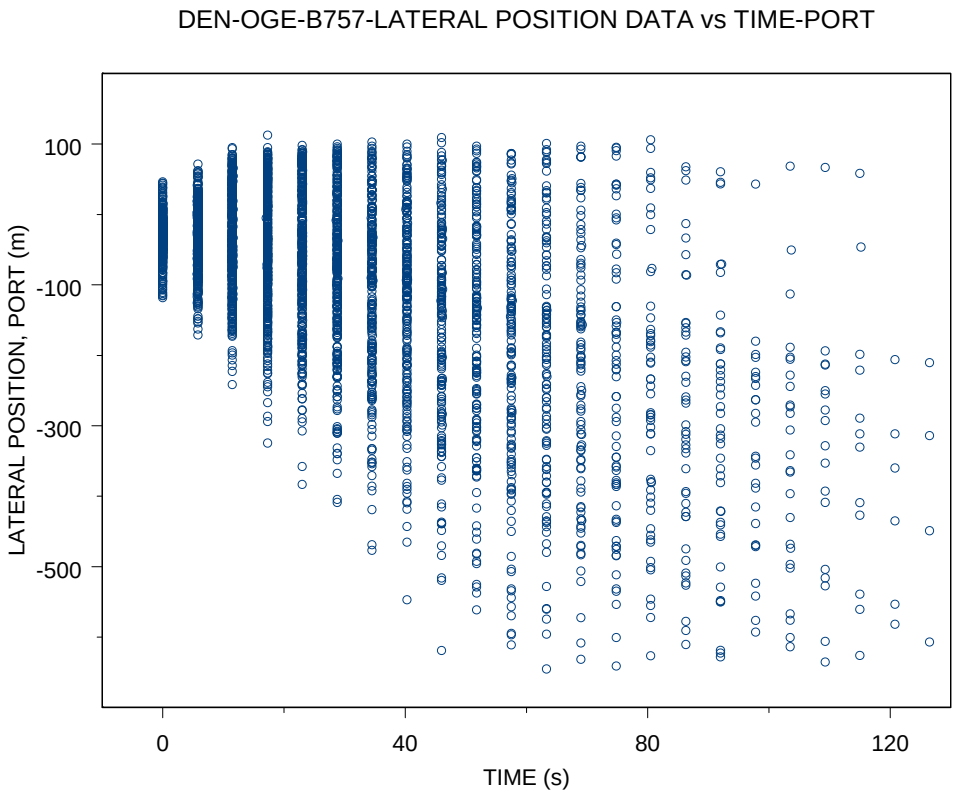

Figure 13. Lateral position data for DEN as a function of time for all B757 OGE landings at DEN. The standard error is 111 m.

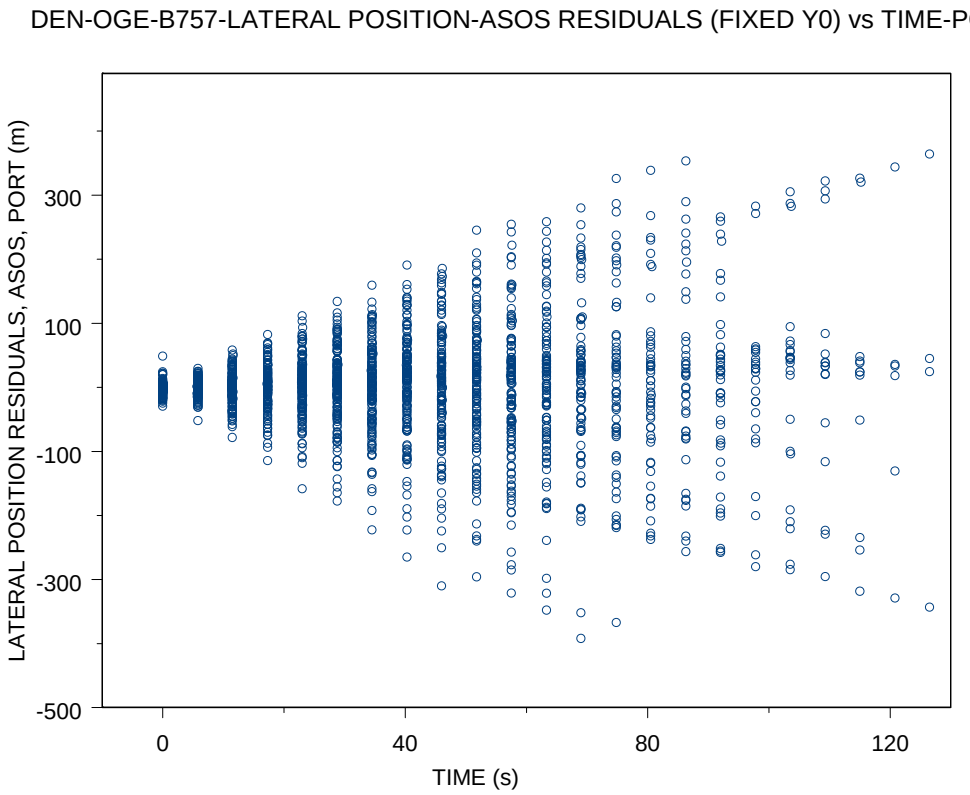

Figure 14. Lateral position residuals using ASOS crosswind, for all B757 OGE landings at DEN with more than 7 points in the port track. For each landing, y_0 was fixed using a 30 s linear estimate. The standard error is 64.8 m.

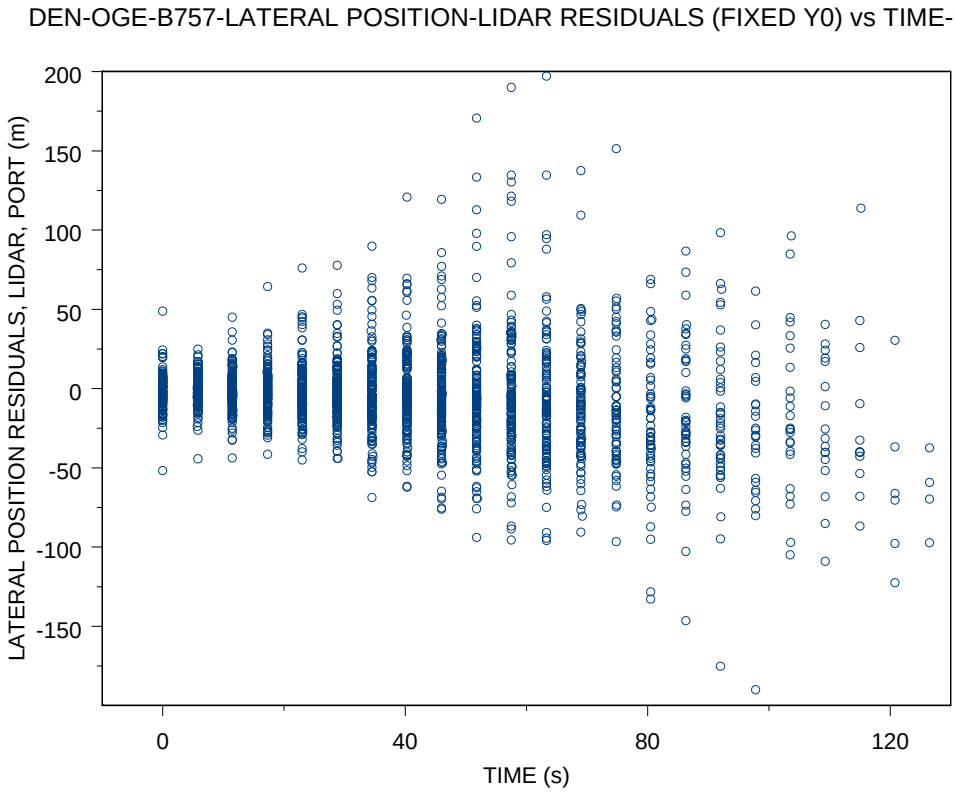

Figure 15. Lateral position residuals using average Lidar crosswind, for all B757 OGE landings at DEN with more than 7 points in the port track. For each landing, y_0 was fixed using a 30 s linear estimate. The standard error is 23.3 m.

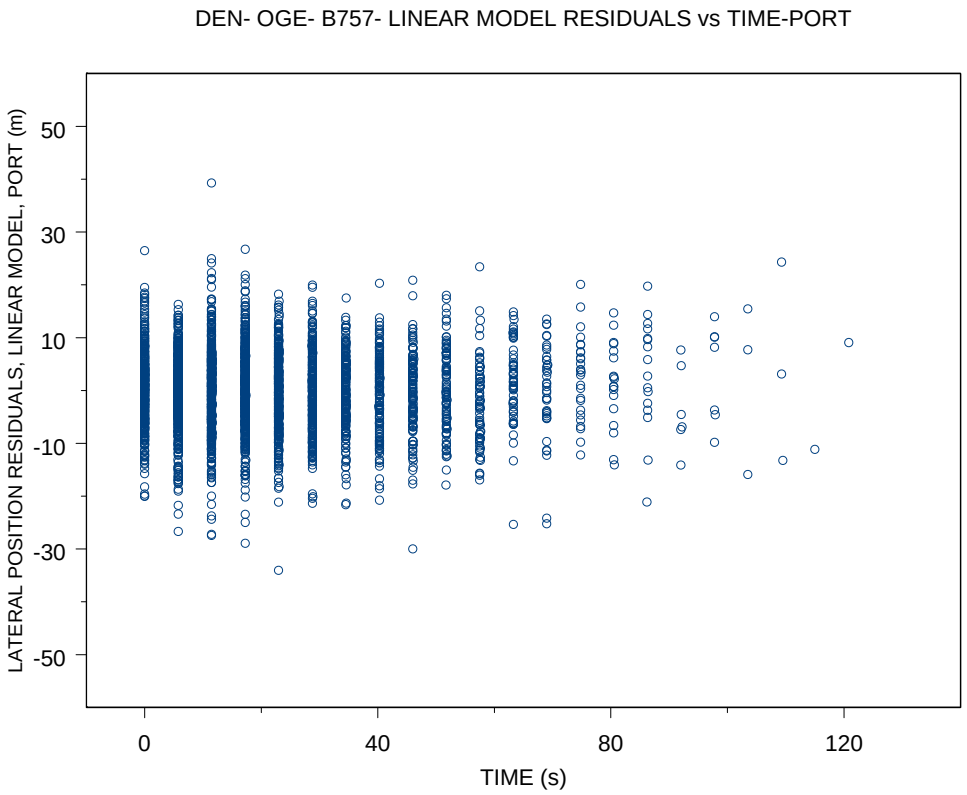

Figure 16. Lateral position residuals using the optimal constant crosswind (the Linear Model) and fixing y_0 for each landing using a 30 s linear fit for all B757 OGE landings at DEN with at least 7 data points in the port track. Note the time independence of the residual spread. The standard error is 7.8 m.

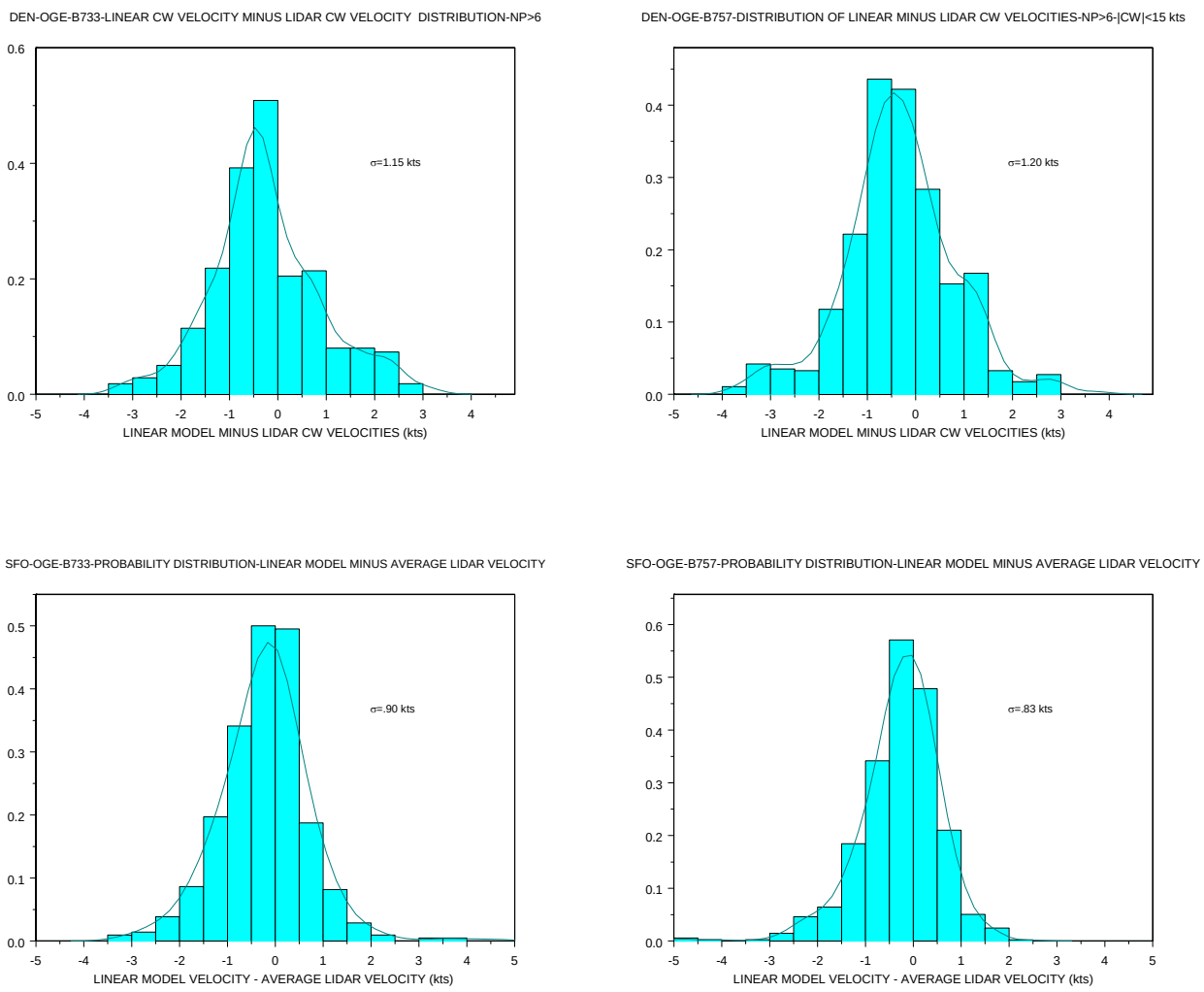

Figure 17. Probability distributions of the difference between Linear Model CW velocity and average Lidar CW velocity for B733 and B757 aircraft. Top left- DEN B733;, top right- DEN B757; bottom left- SFO B733; bottom right- SFO B757. Note that DEN distributions are consistently broader than SFO distributions.

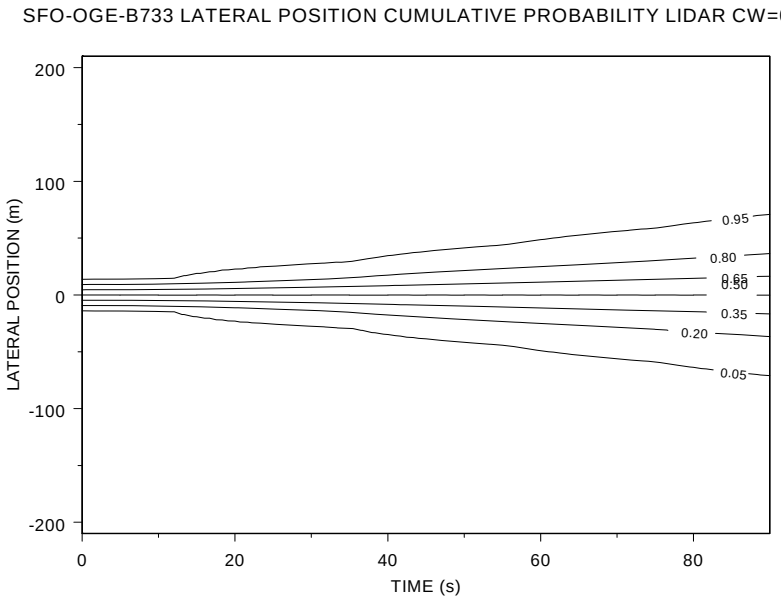

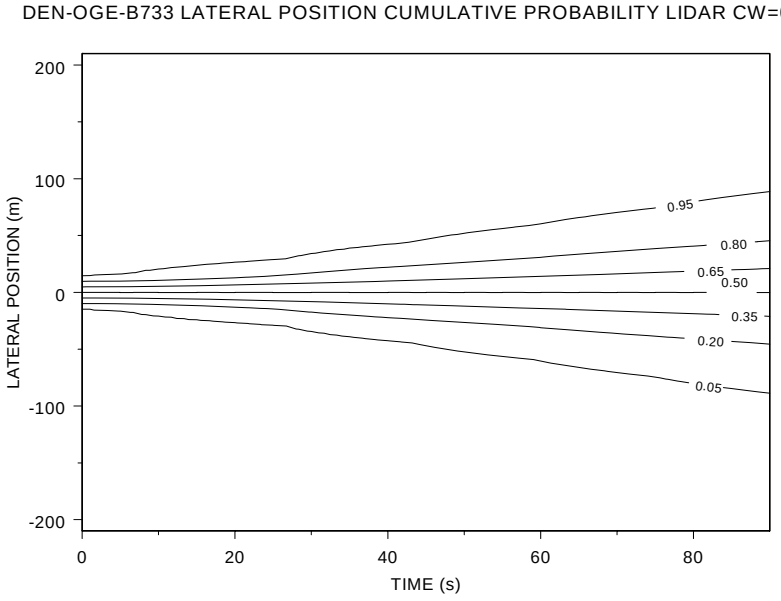

Figure 18a. Cumulative probability distributions for vortex lateral position as a function of time for average Lidar crosswind observation with a CW velocity of 0 kt for B733 OGE aircraft at SFO (top) and DEN (bottom).

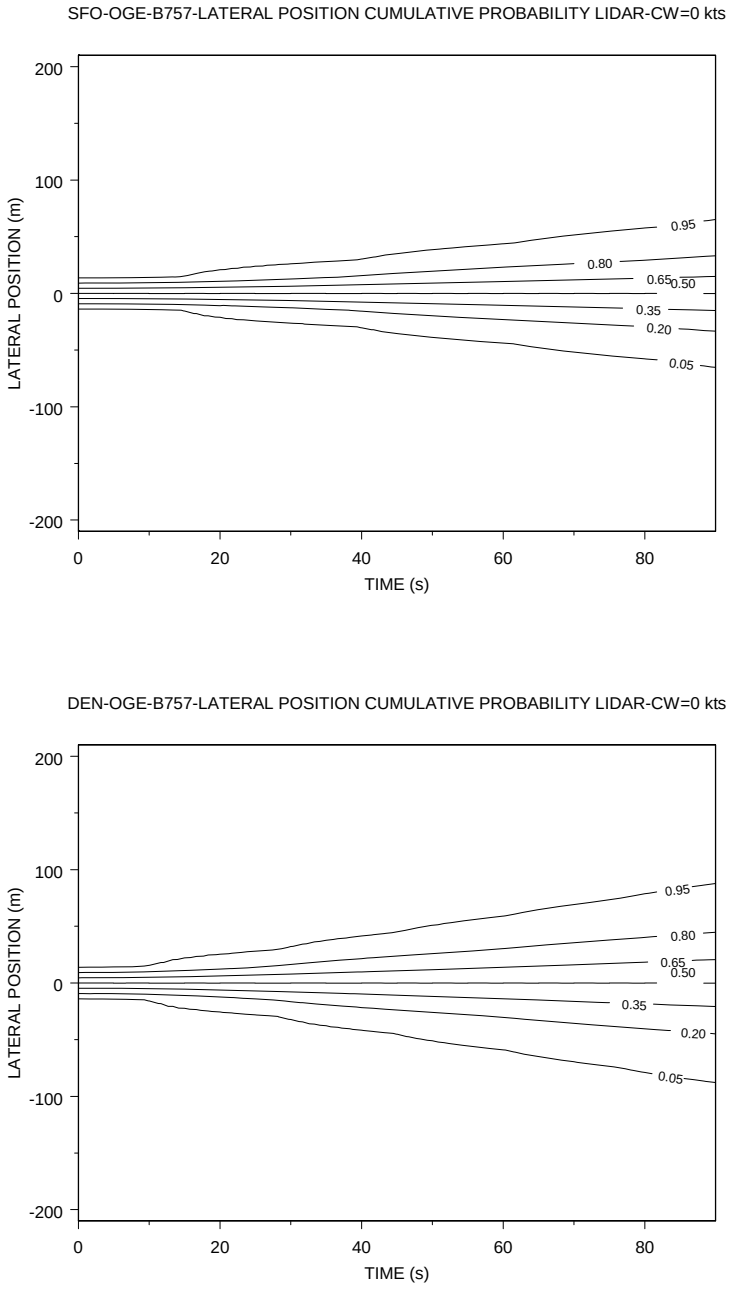

Figure 18b. Cumulative probability distributions for vortex lateral position as a function of time for average Lidar crosswind observation with a CW velocity of 0 kts for B757 OGE aircraft at SFO (top) and DEN (bottom).

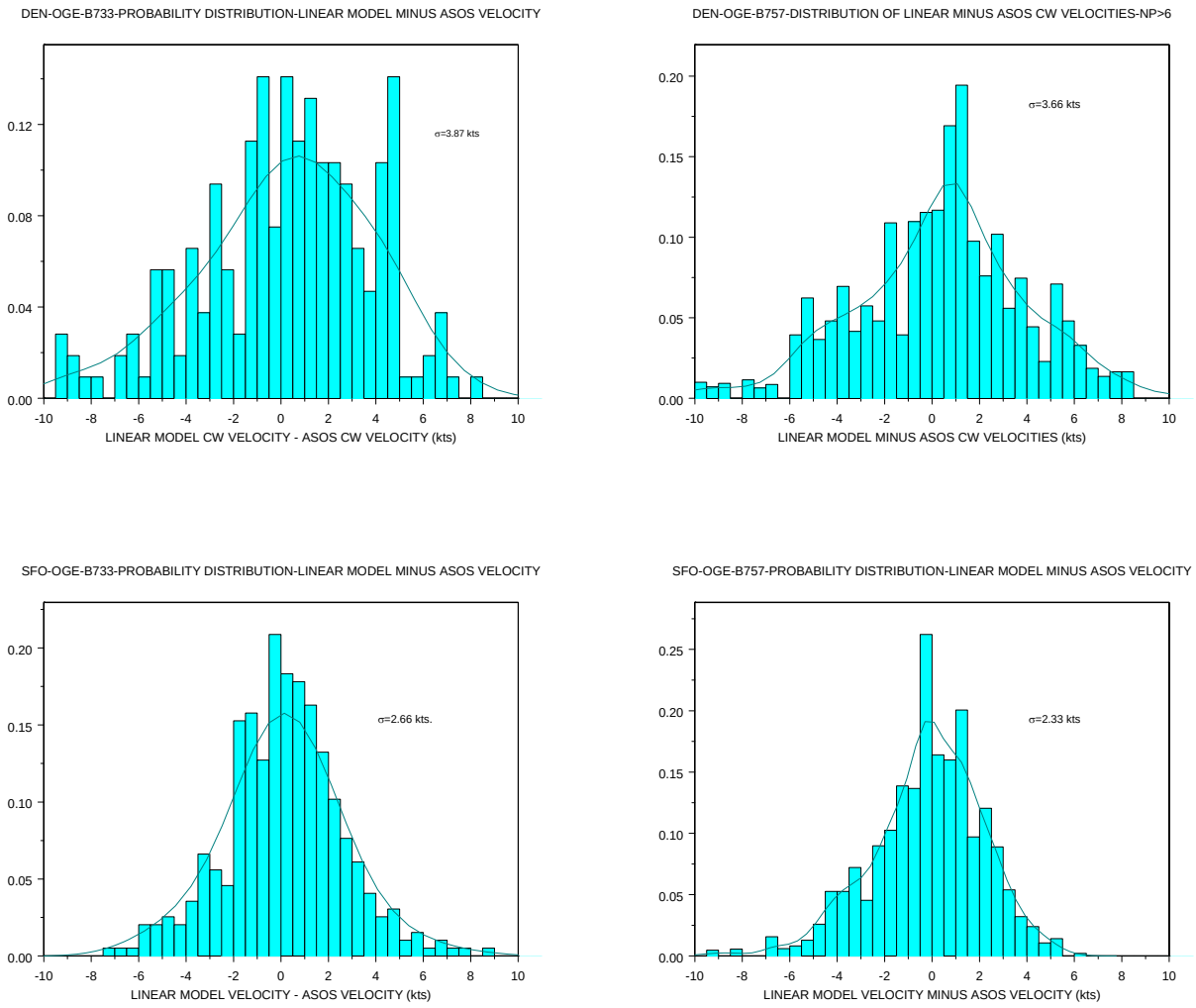

Figure 19. Probability distributions of the difference between Linear Model CW velocity and ASOS CW velocity for B733 and B757 aircraft. Top left- DEN B733; top right- DEN B757; bottom left- SFO B733; bottom right- SFO B757. Note that DEN distributions are consistently broader than the SFO distributions**.**

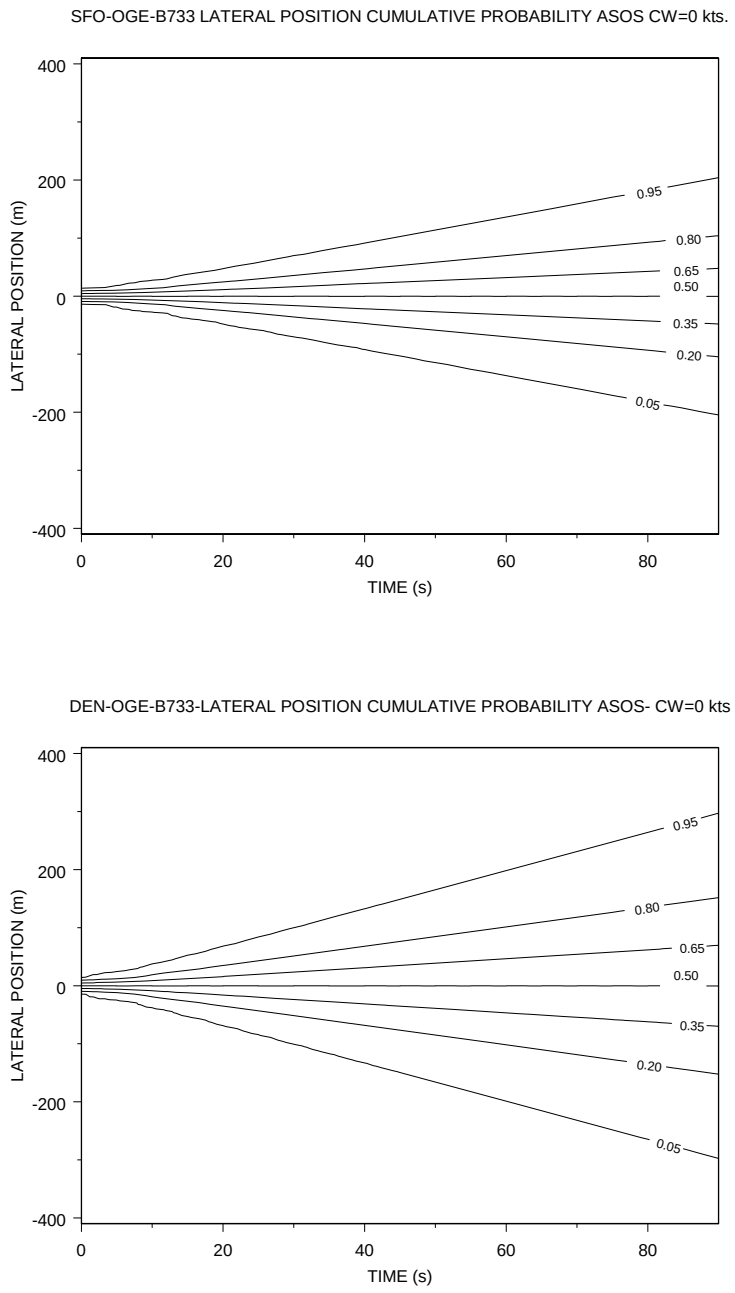

Figure 20a. Cumulative probability distributions for vortex lateral position as a function of time for ASOS crosswind observation with a CW velocity of 0 kts for B733 OGE aircraft at SFO (top) and DEN (bottom). Note the difference in lateral position scale between this figure and Figure 18.

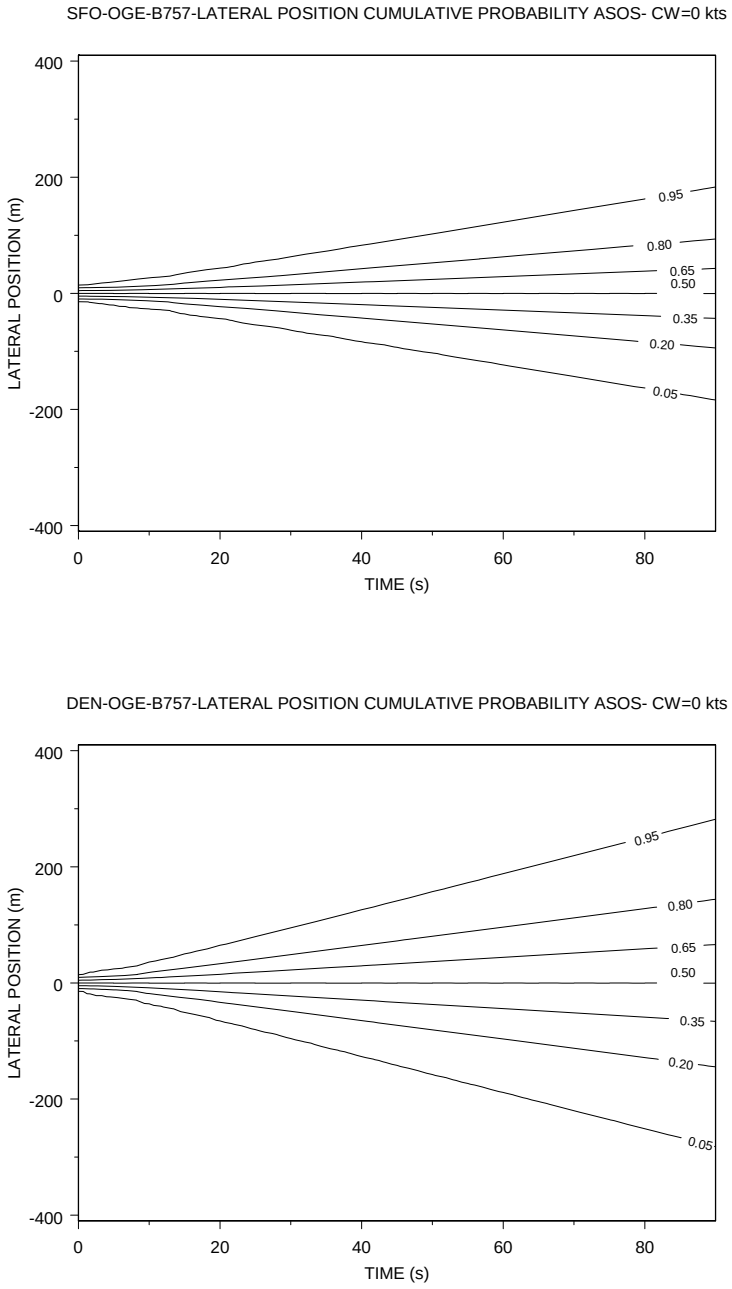

Figure 20b. Cumulative probability distribution for vortex lateral position as a function of time for ASOS crosswind observation with a CW velocity of 0 kts for B757 OGE aircraft at SFO (top) and DEN (bottom). Note the difference in lateral position scale between this figure and Figure 18.

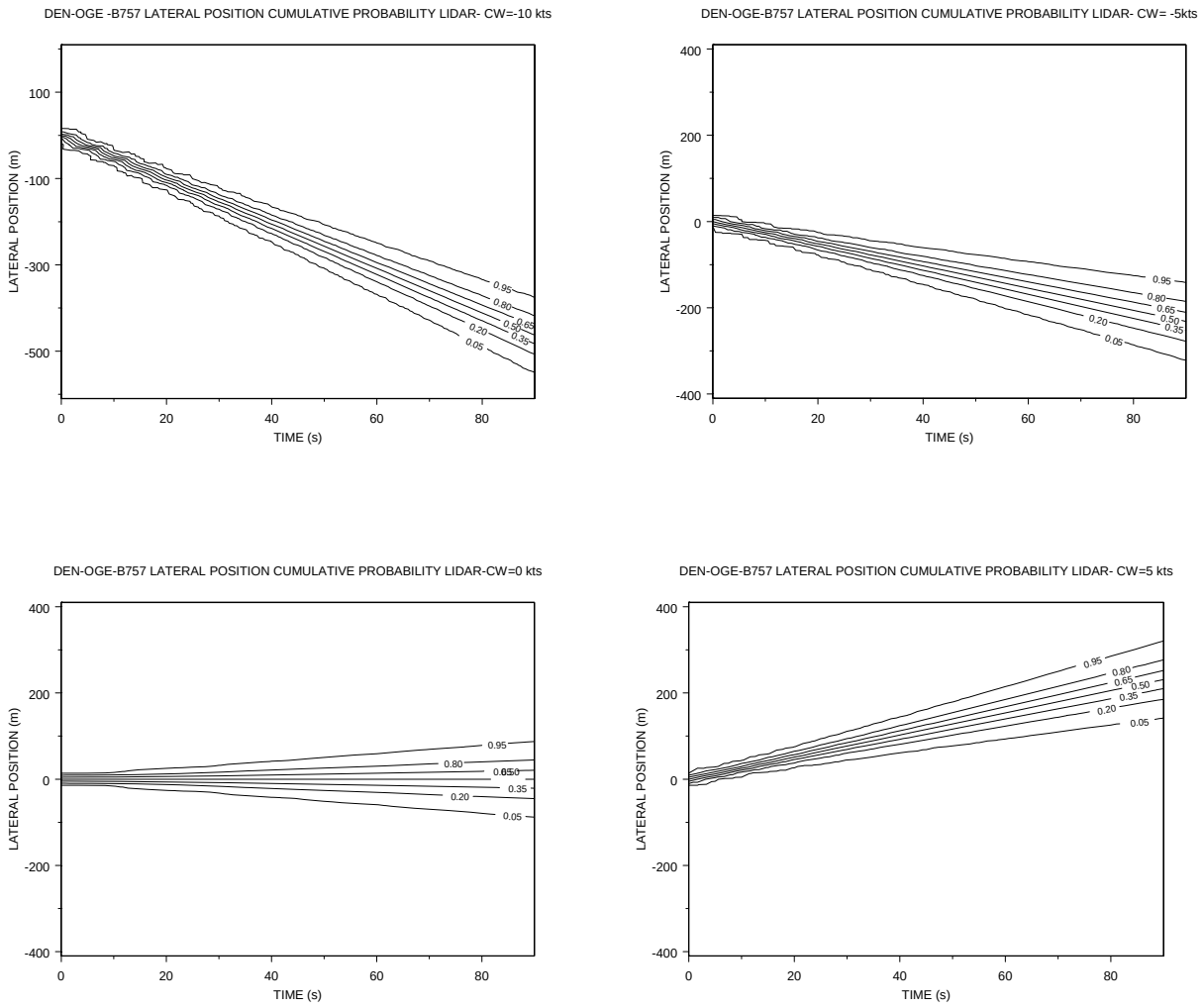

Figure 21. Cumulative probability distributions for lateral position using Lidar observations for varying crosswind velocity at DEN for B757 aircraft.. Top left: -10 kt crosswind velocity. Top right: -5 kt crosswind velocity. Bottom left: 0 kt crosswind velocity. Bottom right: 5 kt crosswind velocity.